Forbidden Electronic Transitions in XeF_2 and XeF_4

EUGENE S. PYSH, JOSHUA JORTNER, AND STUART A. RICE

Department of Chemistry and Institute for the Study of Metals, University of Chicago, Chicago, Illinois 60637

(Received 5 November 1963)

Transition strengths have been measured for the weak 2330 Å band in XeF_2 ($f=0.002$) and for the two weak bands in XeF_4 at 2280 Å ($f=0.009$) and 2580 Å ($f=0.003$). To investigate the origins of these weak transitions, the possibilities of vibronic and singlet–triplet transitions in XeF_2 and XeF_4 were examined. Using the Herzberg–Teller theory of vibronic transitions and a molecular orbital treatment of excited electronic states, estimated strengths of the relevant vibronic transitions have been calculated to be $f=0.001$ for both XeF_2 and XeF_4. The vibronic band in XeF_2 borrows intensity from the symmetry allowed $^1A_{1g}\rightarrow{}^1A_{2u}$ transition at 1580 Å ($f=0.45$), while in XeF_4 the major contribution to the vibronic band is from the symmetry allowed $^1A_{1g}\rightarrow{}^1E_u$ transition at 1325 Å ($f=0.8$). A temperature dependence of the intensity of the 2330 Å band in XeF_2 has been observed and found to be less than that predicted by the Herzberg–Teller theory.

The estimated strength of the singlet–triplet transition in XeF_2 corresponding to the singlet–singlet transition at 1580 Å is shown to be small ($f\leqq 10^{-4}$) in spite of a heavy atom effect; the small transition strength persists because of the lack of nearby excited states of the required symmetry. In XeF_4 the triplet excited state ^3E_u corresponding to the singlet–singlet transition $^1A_{1g}\rightarrow{}^1E_u$ at 1840 Å ($f=0.22$) is permitted by group theoretical selection rules to mix with its own singlet state. Using an intermediate coupling scheme the estimated intensity of this singlet–singlet transition is calculated to be $f=0.007$. The theoretical estimates of the symmetry and spin forbidden transition strengths are used for the assignment of the weak electronic transitions in the xenon fluorides.

I. INTRODUCTION

THE ultraviolet spectra of XeF_2 and XeF_4 have been reported previously.[1,2] In those investigations, the spin and symmetry allowed transitions were classified on the basis of a semiempirical LCAO theory and may be considered to be fairly well understood.[3] This paper is concerned with the nature of the several weak transitions which were also observed.[1–3] Two possibilities are considered herein. First, that the weak transitions are due to symmetry forbidden singlet–singlet transitions which become allowed due to vibronic coupling with u-type molecular vibrations; the general theory of vibronic coupling, due to Herzberg and Teller,[4] is used to calculate the oscillator strengths of the vibronic transitions expected in XeF_2 and XeF_4. Second, we consider the possibility that singlet–triplet transitions are responsible for the observed weak transitions and estimate the expected singlet–triplet transition strengths. Comparison between theory and observation is based on experimental values of the transition strengths determined from a profile analysis of the spectroscopic absorption curves and a study of the temperature dependence of the intensity of the weak XeF_2 band.

II. GENERAL THEORY OF VIBRONIC COUPLING

In recent years several investigators[5–8] have used the Herzberg–Teller theory for estimating the strength of vibrational induced electronic transitions. Benzene[5–7] has been the most widely studied molecule, but calculations have been reported for formaldehyde[8] and certain transition metal complexes.[9–11] In this work a charge-dipole model was used in a molecular orbital framework. Pople and Sidman[8] have used this combination successfully to calculate the intensity of the $^1A_1\rightarrow{}^1A_2(n\rightarrow\pi^*)$ transition in formaldehyde. In the following we give a brief general summary of the theory as it is used in this paper.

In the Born–Oppenheimer approximation, the vibronic wavefunction of a molecule is expressed in the form

$$\Psi_{kj}=\Theta_k(x,q)\Phi_{kj}(q), \tag{1}$$

where x and q refer to the complete set of coordinates required to locate all of the electrons and nuclei, respectively, $\Theta_k(x,q)$ is the electronic wavefunction of the kth electronic state for fixed q, and $\Phi_{kj}(q)$ is the vibrational wavefunction of the jth vibrational state

[1] E. G. Wilson, J. Jortner, and S. A. Rice, J. Am. Chem. Soc. **85,** 813 (1963).
[2] J. Jortner, E. G. Wilson, and S. A. Rice, J. Am. Chem. Soc. **85,** 815 (1963).
[3] J. Jortner, E. G. Wilson, and S. A. Rice, *Noble Gas Compounds* (University of Chicago Press, Chicago, 1963), p. 358.
[4] G. Herzberg and E. Teller, Z. Physik. Chem. (Leipzig) **B21,** 410 (1933).
[5] J. N. Murrell and J. A. Pople, Proc. Phys. Soc. (London) **A69,** 245 (1956).
[6] A. D. Liehr, Can. J. Phys. **35,** 1123 (1957); **36,** 1588 (1957).
[7] A. C. Albrecht, J. Chem. Phys. **33,** 156, 169 (1960).
[8] J. A. Pople and J. W. Sidman, J. Chem. Phys. **27,** 1270 (1957).
[9] O. G. Holms and D. S. McClure, J. Chem. Phys. **25,** 1686 (1957).
[10] C. J. Ballhausen and A. D. Liehr, Phys. Rev. **106,** 1161 (1957).
[11] R. Engleman, Mol. Phys. **3,** 48 (1960).

of electronic state k. The coordinates q are taken to be zero at equilibrium.

The substitution of the right-hand side of Eq. (1) into the general expression for the transition moment $\mathbf{M}_{gi,kj}$ between vibronic states described by the quantum numbers gi, kj gives

$$\mathbf{M}_{gi,kj}=\int \Phi_{gi}^*(q)\mathbf{M}_{gk}(q)\Phi_{kj}(q)\,dq, \tag{2}$$

where

$$\mathbf{M}_{gk}(q)=\int \Theta_g^*(x,q)\mathbf{m}_e(x)\Theta_k(x,q)\,dx \tag{3}$$

is the variable electronic transition moment, g denotes the ground state, and $\mathbf{m}_e$ is the electronic contribution to the electric dipole moment operator. The contribution of the nuclear term to the transition moment operator vanishes by virtue of orthogonality relations. The total transition probability from state g to state k, invoking the quantum-mechanical sum rule, is found to be

$$f_{k\leftarrow g}=\frac{8\pi^2 mc}{3h^2e^2}E_{k\leftarrow g}\sum_i B_i\sum_j |\mathbf{M}_{gi,kj}|^2,$$

$$=\frac{8\pi^2 mc}{3h^2e^2}E_{k\leftarrow g}\sum_i B_i\int \Phi_{gi}^*(q)\mathbf{M}_{gk}^2(q)\Phi_{gi}(q)\,dq, \tag{4}$$

where B_i is the Boltzmann weighting factor for vibrational state i and $E_{k\leftarrow g}$ represents a mean transition energy.

In the Herzberg–Teller theory it is assumed that the electronic wavefunction can be expanded in the following form:

$$\Theta_k(x,q)=\Theta_k^0(x)+\sum_s \lambda_{ks}(q)\Theta_s^0(x), \tag{5}$$

where $\Theta_k^0(x)$ is the ground state electronic wavefunction for the molecule in the equilibrium nuclear configuration and the summation is over all excited states s. The coefficients cited above are given by perturbation theory in the form

$$\lambda_{ks}(q)=\frac{1}{E_{k\leftarrow g}-E_{s\leftarrow g}}\int \Theta_k^0(x)H'(q)\Theta_s^0(x)\,dx, \tag{6}$$

where $H'(q)$ is the perturbation Hamiltonian. Then, from Eqs. (3) and (5),

$$\mathbf{M}_{gk}(q)=\mathbf{M}_{gk}^0+\sum_s \lambda_{ks}(q)\mathbf{M}_{gs}^0+\sum_t \lambda_{gt}(q)\mathbf{M}_{tk}^0. \tag{7a}$$

We are interested in the cases where $\mathbf{M}_{gk}^0$ vanishes. We also assume that the ground state does not mix appreciably under vibronic perturbation, so that the final summation also vanishes. Equation (7a) then reduces to

$$\mathbf{M}_{gk}(q)=\sum_s \lambda_{ks}(q)\mathbf{M}_{gs}^0. \tag{7b}$$

In order that $\mathbf{M}_{gk}(q)$ be nonvanishing, some $\lambda_{ks}(q)$ and $\mathbf{M}_{gs}^0$ must be nonvanishing. A nonvanishing $\mathbf{M}_{gs}^0$ requires the purely electronic transition to be allowed under spin and symmetry selection rules. A nonvanishing $\lambda_{ks}(q)$ requires the integral in Eq. (6) to form the basis of a representation which contains at least once the totally symmetric irreducible representation of the group of the molecule. This latter requirement may be used to determine which vibrations are capable of mixing two electronic states of known symmetry.

For small vibrations the perturbation Hamiltonian may be expanded in powers of the nuclear displacement coordinate q. For each normal vibration a, when nonlinear terms are dropped,

$$H'(q)_a=q_a(\partial H/\partial q_a). \tag{8}$$

Replacing the effective Hamiltonian, H, by a Coulomb potential and carrying out a transformation from normal to Cartesian coordinates one obtains

$$H'(q)_a=-q_a(\partial/\partial q_a)\sum_i\sum_\sigma (Z_\sigma e^2/r_{i\sigma})$$

$$=q_a\sum_i\sum_\sigma Z_\sigma e^2(\partial \mathbf{r}_\sigma/\partial q_a)_0(\mathbf{r}_{i\sigma}/r_{i\sigma}^3). \tag{9}$$

In Eq. (9) the electrons are labeled by i, the nuclei by σ, and $\mathbf{r}_{i\sigma}$ is the vector from electron i to nucleus σ. The derivatives $(\partial \mathbf{r}_\sigma/\partial q_a)_0$ are evaluated for the ground state and are the elements of the matrix which transforms from normal coordinates to Cartesian displacement coordinates.

Using Eqs. (4), (6), (7), and (9) and carrying out the summation over vibrational levels the general expression for the oscillator strength of a "forbidden" band may be written in terms of the characteristics of the intense bands from which it borrows intensity:

$$f_{k\leftarrow g}=\sum_s f_{s\leftarrow g}\frac{E_{k\leftarrow g}}{E_{s\leftarrow g}(E_{k\leftarrow g}-E_{s\leftarrow g})^2}\sum_a \coth\frac{h\nu_a}{2kT}(W_{ks})_a^2, \tag{10}$$

where W_{ks} is the vibrational–electronic interaction energy matrix element between the electronic states k and s. For each normal mode of vibration a, the contribution to W_{ks} is given by

$$(W_{ks})_a=\int \Theta_k^0(x)\left[\sum_\sigma\sum_i Z_0e^2\left(\frac{\partial \mathbf{r}_\sigma}{\partial q_a}\right)_0\frac{\mathbf{r}_{i\sigma}}{r_{i\sigma}^3}\langle Q_a^2\rangle_{Av}^{\frac{1}{2}}\right]\Theta_s^0(x)\,dx, \tag{11}$$

where $\langle Q_a^2\rangle_{Av}^{\frac{1}{2}}$ is the root mean square displacement of the normal coordinate of the ath normal mode in the zeroth vibrational state of the ground electronic state. The temperature-dependent factor in Eq. (10) arises from the application of the harmonic oscillator approximation to the ground and excited states.[7,10,11]

All the terms in Eq. (10) except $(W_{ks})_a$ may be evaluated empirically. When molecular orbital theory

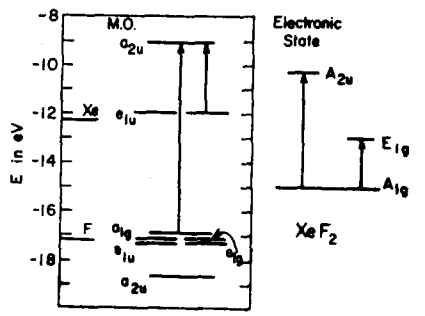

FIG. 1. Molecular orbital energy-level diagram for XeF_2 showing symmetry-allowed and vibronic transitions.

is used to represent the electronic wavefunction Eq. (11) can be simplified, since the expression in brackets is a one-electron operator. The matrix element therefore vanishes if the configurations of Θ_k^0 and Θ_s^0 differ in more than one molecular orbital. Equation (11) can then be written in the form

$$(W_{ks})_a=\int\psi_1(x)\left[\sum_\sigma Z_\sigma e^2\left(\frac{\partial \mathbf{r}_\sigma}{\partial q_a}\right)_0\frac{\mathbf{r}_{i\sigma}}{r_{i\sigma}^3}\langle Q_a^2\rangle_{Av}^{\frac{1}{2}}\right]\psi_2(x)\,dx, \quad (12)$$

where ψ_1 and ψ_2 are the unmatched molecular orbitals in Θ_s^0 and Θ_k^0. In the following calculations Eq. (12) was represented by the interaction energy between a set of dipoles, $\mathfrak{y}_\sigma$, defined by

$$\mathfrak{y}_\sigma=Z_\sigma e(\partial \mathbf{r}_\sigma/\partial q_a)_0\langle Q_a^2\rangle_{Av}^{\frac{1}{2}} \quad (13)$$

and the electron density distribution, $e\psi_1\psi_2$.

In the harmonic oscillator approximation to the vibrational wavefunction, $\langle Q_a^2\rangle_{Av}^{\frac{1}{2}}$ is found to be

$$\langle Q_a^2\rangle_{Av}^{\frac{1}{2}}=(h/8\pi^2\nu_a)^{\frac{1}{2}}. \quad (14)$$

The quantities $(\partial \mathbf{r}_\sigma/\partial q_a)_0$, obtained from a normal coordinate analysis, are the elements of the matrix $[\mathbf{M}^{-1}\mathbf{B}^\dagger(\mathbf{L}^{-1})^\dagger]$. The elements of the diagonal matrix $\mathbf{M}$ are the relevant atomic masses. $\mathbf{B}$ is the matrix which transforms from Cartesian to symmetry coordinates and $\mathbf{L}$ is the matrix which transforms from normal to symmetry coordinates.[12] $\mathbf{L}$ is further defined by the following matrix equation:

$$\mathbf{L}^\dagger\mathbf{F}\mathbf{G}=\mathbf{\Lambda}\mathbf{L}^\dagger,$$
$$\mathbf{G}=\mathbf{L}\mathbf{L}^\dagger, \quad (15)$$

where $\mathbf{F}$ and $\mathbf{G}$ refer to Wilson's potential and kinetic energy matrices. All the matrices can be evaluated by standard methods.[12]

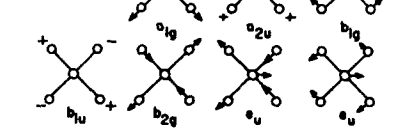

FIG. 2. Normal vibrations of (a) XeF_2, point group $D_{\infty h}$ and (b) XeF_4, point group D_{4h}.

III. VIBRONIC COUPLING IN XENON DIFLUORIDE

Figure 1 displays the results of a semiempirical LCAO molecular orbital treatment of the XeF_2 molecule.[3] An intense absorption band at 1580 Å ($f=0.45$) is ascribed to a singlet–singlet $^1A_{1g}\rightarrow{}^1A_{2u}$ transition representing the transfer of an electron from the a_{1g} molecular orbital, made up mostly of fluorine $2p$ sigma orbitals, to the nonbonding a_{2u} molecular orbital, made up mostly of the xenon $5p$ sigma orbital. The symmetry forbidden transition $^1A_{1g}\rightarrow{}^1E_{1g}$ corresponding to an excitation of an electron from the e_{1u} molecular orbital to the a_{2u} molecular orbital would become allowed by mixing of the $^1A_{2u}$ and $^1E_{1g}$ excited states. From the symmetry requirements placed on the perturbation Hamiltonian by the considerations following Eq. (7b) mixing of the $^1A_{2u}$ and $^1E_{1g}$ excited states is possible only by interaction with the doubly degenerate bending vibration, Π_u [see Fig. 2(a)].

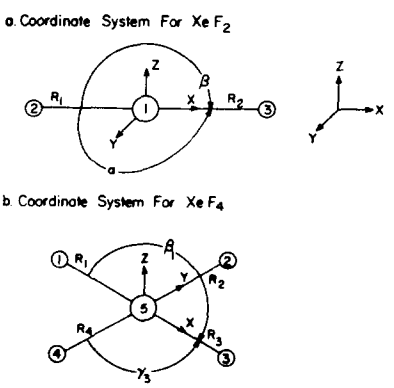

FIG. 3. Cartesian coordinates and internal coordinates for (a) XeF_2 and (b) XeF_4.

Figure 3(a) defines the Cartesian coordinate system used herein. The internal coordinates are the changes in bond lengths and bond angles in the xy and xz planes:

$$\Delta R_1=x_1-x_2,$$
$$\Delta R_2=-x_1+x_3,$$
$$\Delta\alpha=-(2y_1/r_0)+(y_2/r_0)+(y_3/r_0),$$
$$\Delta\beta=-(2z_1/r_0)+(z_2/r_0)+(z_3/r_0), \quad (16)$$

where r_0 is the XeF_2 equilibrium internuclear distance.[13]

[12] E. B. Wilson, J. C. Decius, and P. C. Cross, *Molecular Vibrations* (McGraw-Hill Book Company, Inc., New York, 1955).

[13] P. A. Agron, G. M. Begun, H. A. Levy, A. A. Mason, C. G. Jones, and D. F. Smith, Science **139**, 842 (1963).

TABLE I. **B** matrix for XeF_2.

	Xe			F_2			F_3		
	x	y	z	x	y	z	x	y	z
$S(\Sigma_g^+)$	0	0	0	−0.7071	0	0	+0.7071	0	0
$S(\Sigma_u^+)$	1.414	0	0	−0.7071	0	0	−0.7071	0	0
$S(\Pi_u)$	0	-1.0×10^8	0	0	0.50×10^8	0	0	0.50×10^8	0

The corresponding symmetry coordinates are

$$S(\Sigma_g^+)=(1/\sqrt{2})(\Delta R_1+\Delta R_2),$$
$$S(\Pi_u)=\Delta\alpha,$$
$$S(\Sigma_u^+)=(1/\sqrt{2})(\Delta R_1-\Delta R_2). \quad (17)$$

The **B** matrix and potential energy matrix, **F**, are obtained by standard methods. They are shown in Table I and Table II, respectively. F_r is the bond stretching force constant, F_r' is the interaction force constant, and F_α is the angle bending force constant. The elements of the kinetic energy matrix, **G**, can be evaluated from Wilson's tables.[12] Solving the matrix Eq. (15) yields the matrix $\mathbf{L}^{-1}$: its elements are found to be

$$Q_1=0.5618\times10^{-11}S(\Sigma_g^+),$$
$$Q_2=0.6988\times10^{-19}S(\Pi_u),$$
$$Q_3=0.4941\times10^{-11}S(\Sigma_u^+). \quad (18)$$

Table III displays the values of $(\partial\mathbf{r}_\sigma/\partial q_a)_0$ for the three normal vibrations. Only that column referring to the Π_u vibration is relevant to our calculations ($\nu=213$ cm^{-1}).[13] Also given in Table III are the values of the rms displacements, $\langle Q_a^2\rangle^{\frac{1}{2}}$, calculated from Eq. (14). By a simple transformation of coordinates, the xenon atom was considered fixed and the resulting vibration dipole on each fluorine atom was calculated. Equation (13) with Z equal to unity gives

$$\mu_F=0.096\ ea_0 \text{ (in } y \text{ direction)}$$
and
$$\mu_F=0.096\ ea_0 \text{ (in } z \text{ direction)}. \quad (19)$$

As mentioned previously, these dipoles were considered to interact with a charge density on the stationary xenon atom. To evaluate the charge density, $e\psi(a_{1g})\psi(e_{1u})$ analytic representations of the molecular orbitals are needed. $\psi(a_{1g})$ was considered to be of the form

$$\psi(a_{1g})=(a/\sqrt{2})[\phi(2p_xF_1)+\phi(2p_xF_2)]+(b/\sqrt{2})[\phi(2sF_1)+\phi(2sF_2)]+c\phi(5s\mathrm{Xe}). \quad (20)$$

Solutions to the secular equation were obtained using the same approximations as employed in an earlier study.[3] The coefficients were found to be: $a=-0.747$, $b=-0.171$, and $c=0.518$. $\psi(e_{1u})$ was considered to be of the form

$$\psi(e_{1u})=\alpha\begin{Bmatrix}\phi(5p_y\mathrm{Xe})\\ \phi(5p_z\mathrm{Xe})\end{Bmatrix}+\beta\begin{Bmatrix}\phi(2p_yF_1)+\phi(2p_yF_2)\\ \phi(2p_zF_1)+\phi(2p_zF_2)\end{Bmatrix}. \quad (21)$$

From Ref. 3, $\alpha=-0.284$ and $\beta=0.977$. To evaluate the charge density $e\psi(a_{1g})\psi(e_{1u})$ the molecular orbitals were expanded in terms of the component atomic orbitals. Contributions in the expansion similar to overlap terms (i.e., two-center integrals) were neglected. Of the remaining contributions, only those transforming like dipoles were kept since the interaction of vibration dipoles with quadrupole charge densities will be much smaller than the term retained. Expanding the molecular orbitals in this way yields

$$\psi(a_{1g})\psi(e_{1u})=0.547\phi(5s\mathrm{Xe})\phi(5p_y\mathrm{Xe})+0.547\phi(5s\mathrm{Xe})\phi(5p_z\mathrm{Xe}). \quad (22)$$

The atomic charge distributions are approximated by a point dipole of moment $e\langle\phi(5s\mathrm{Xe})\,|\,\mathbf{r}\,|\,\phi(5p_a\mathrm{Xe})\rangle$,

TABLE II. Potential-energy matrix for XeF_2

$S(\Sigma_g^+)$	$S(\Sigma_u^+)$	$S(\Pi_u)$
F_R+F_R'	0	0
	F_R-F_R'	0
		F_β

TABLE III. Values of $(\partial r/\partial q_a)_0$ and $\langle Q^2\rangle^{\frac{1}{2}}$ for XeF_2.[a]

		Σ_g^+	Σ_u^+	Π_u
Xe	x	0	0.0417	0
	y	0	0	−0.0417
	z	0	0	0
F_2	x	−0.1623	−0.1428	0
	y	0	0	+0.1428
	z	0	0	0
F_3	x	+0.1623	−0.1428	0
	y	0	0	+0.1428
	z	0	0	0
$\langle Q^2\rangle^{\frac{1}{2}}$		0.1808	0.1738	0.2809

[a] Values of $(\partial r/\partial q_a)_0$ are multiplied by $N^{-\frac{1}{2}}$ where N is Avogadro's number. Values of $\langle Q^2\rangle^{\frac{1}{2}}$ are multiplied by $N^{\frac{1}{2}}$.

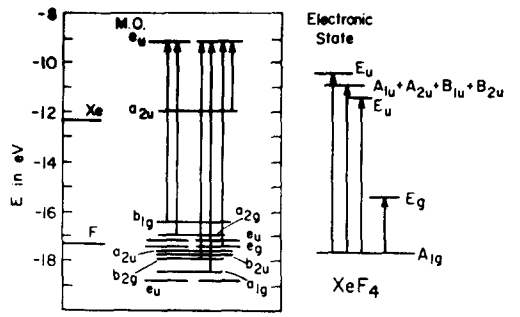

FIG. 4 Molecular orbital energy-level diagram for XeF_4 showing symmetry-allowed and vibronic transitions.

where α is y or z. The atomic orbitals used were of the Slater type, i.e.:

$$\phi(5s\mathrm{Xe}) = 0.826r^3 \exp(-2.0625r),$$
$$\phi(5p_\alpha\mathrm{Xe}) = 1.431r^3 \exp(-2.0625r)\cos\theta_\alpha. \quad (23)$$

$\langle\phi(5s\mathrm{Xe}) \mid \mathbf{r} \mid \phi(5p_\alpha\mathrm{Xe})\rangle$ is then calculated to be 1.26 ea_0 in the α direction.

The classical interaction energy of the vibration dipoles with the charge density leads to $(W_{ks})\Pi_u = 0.0639$ eV. This value is substituted into Eq. (10) together with the following empirical data from Ref. 3:

$$E(E_{1g}\leftarrow A_{1g}) = 5.4 \text{ eV},$$
$$E(A_{2u}\leftarrow A_{1g}) = 7.9 \text{ eV},$$
$$f(A_{2u}\leftarrow A_{1g}) = 0.45, \quad (24)$$

so that at $T = 303°\mathrm{K}$,

$$f(E_{1g}\leftarrow A_{1g})\,(\mathrm{est}) = 0.001. \quad (25)$$

IV. VIBRONIC COUPLING IN XENON TETRAFLUORIDE

Figure 4 displays the results of a semiempirical LCAO molecular orbital treatment of the XeF_4 molecule.[3] The absorption band at 1840 Å ($f=0.22$) is ascribed to two singlet–singlet symmetry allowed transitions. One represents the transfer of an electron from a sigma b_{1g} molecular orbital to the antibonding e_u molecular orbital and the other from a pi-type a_{2g} molecular orbital to the same orbital. Both of these transitions are described as $^1A_{1g}\rightarrow {}^1E_u$. The intensity of the second strong absorption band at 1325 Å ($f=0.80$) is similarly ascribed to two symmetry allowed singlet–singlet transitions, one representing excitation from the a_{1g} sigma-type molecular orbital and the other from a pi-type b_{2g} molecular orbital. Both of these transitions are also described as $^1A_{1g}\rightarrow {}^1E_u$. The expected pi–sigma transition from the e_g molecular orbital to the e_u antibonding molecular orbital was not definitely assigned to an experimental band.

One discrete weak band and traces of a second are found on the high wavelength side of the 1840-Å band. One of these could result from the symmetry forbidden $^1A_{1g}\rightarrow {}^1E_g$ transition corresponding to the excitation from the a_{2u} highest filled molecular orbital to the antibonding e_u molecular orbital. Such a transition could gain intensity either by mixing the ^1E_g state with ^1E_u by either the a_{2u} or b_{1u} out of plane normal vibrations or by mixing the ^1E_g state and $^1A_{1u}+{}^1A_{2u}+{}^1B_{1u}+{}^1B_{2u}$ state with the two e_u normal vibrations [see Fig. 2(b)].

The reducible representation of the molecular vibrations can be expressed in terms of the irreducible representations of D_{4h}.

$$\Gamma = A_{1g}+A_{2u}+B_{1g}+B_{1u}+B_{2g}+2E_u.$$

Figure 3(b) defines the Cartesian coordinate system used in this case. The internal coordinates defined were the changes in the bond lengths R, the changes in the in-plane bond angles γ, and the changes in the out of plane bond angles β, where β_1 is the F_1–Xe–F_3 angle in the plane perpendicular to the XeF_2 bond, and β_2 is the F_2–Xe–F_4 angle in the plane perpendicular to the XeF_1 bond. r_0 is the internuclear distance.[14] We find

$$\Delta R_1 = -x_1+x_5,$$
$$\Delta R_2 = y_2-y_5,$$
$$\Delta R_3 = x_3-x_5,$$
$$\Delta R_4 = -y_4+y_5,$$
$$\Delta\gamma_1 = -y_1/r_0+x_2/r_0-x_5/\sqrt{2}r_0+y_5/\sqrt{2}r_0,$$
$$\Delta\gamma_2 = -x_2/r_0-y_3/r_0+x_5/\sqrt{2}r_0+y_5/\sqrt{2}r_0,$$
$$\Delta\gamma_3 = y_3/r_0-x_4/r_0+x_5/\sqrt{2}r_0-y_5/\sqrt{2}r_0,$$
$$\Delta\gamma_4 = y_1/r_0+x_4/r_0-x_5/\sqrt{2}r_0-y_5/\sqrt{2}r_0,$$
$$\Delta\beta_1 = -z_1/r_0-z_3/r_0+2z_5/r_0,$$
$$\Delta\beta_2 = -z_2/r_0-z_4/r_0+2z_5/r_0, \quad (26)$$

leading to the following symmetry coordinates:

$$S(A_{1g}) = \tfrac{1}{2}(\Delta R_1+\Delta R_2+\Delta R_3+\Delta R_4),$$
$$S(A_{2u}) = (1/\sqrt{2})\,(\Delta\beta_1+\Delta\beta_2),$$
$$S(B_{1g}) = \tfrac{1}{2}(\Delta\gamma_1-\Delta\gamma_2+\Delta\gamma_3-\Delta\gamma_4),$$
$$S(B_{1u}) = (1/\sqrt{2})\,(\Delta\beta_2-\Delta\beta_1),$$
$$S(B_{2g}) = \tfrac{1}{2}(\Delta R_1-\Delta R_2+\Delta R_3-\Delta R_4),$$
$$S(E_u)_R = \tfrac{1}{2}(\Delta R_1-\Delta R_2-\Delta R_3+\Delta R_4),$$
$$S(E_u)_\gamma = (1/\sqrt{2})\,(\Delta\gamma_2-\Delta\gamma_4). \quad (27)$$

These symmetry coordinates are normalized and mutually orthogonal and transform according to the character table of the symmetry point group D_{4h}.

The **B** matrix and **F** matrix obtained are shown in Table IV and Table V, respectively. The independent

[14] H. H. Claassen, C. L. Chernick, and J. G. Malm, J. Am. Chem. Soc. **85**, 1927 (1963).

constants in the potential energy matrix are defined as follows:

F_r, bond stretching constant; F_r', interaction constant of a bond with a bond at right angles to it; F_r'', interaction constant of a bond with an opposite bond; F_γ, interbond angle constant for γ angles; F_γ', interaction constant of two adjacent angles in the plane of the molecule; F_γ'', interaction constant of two nonadjacent angles in the plane of the molecule; F_β, interbond angle constant for β angles; F_β', interaction constant of the two β angles; $F_{r\gamma}$, interaction constant of a bond with an angle adjacent to it; $F_{r\gamma}'$, interaction constant of a bond with a nonadjacent angle.

The elements of the **G** matrix were evaluated and found to be:

$$G(A_{1g}) = \mu_F,$$
$$G(A_{2u}) = (2\mu_F/r_0^2) + (8\mu_{Xe}/r_0^2),$$
$$G(B_{1g}) = 4\mu_F/r_0^2,$$
$$G(B_{1u}) = 2\mu_F/r_0^2,$$
$$G(B_{2g}) = \mu_F,$$
$$G(E_u)_R = \mu_F + 2\mu_{Xe},$$
$$G(E_u)_\gamma = (2\mu_F/r_0^2) + (4\mu_{Xe}/r_0^2),$$
$$G(E_u)_{R\gamma} = -2\sqrt{2}\mu_{Xe}/r_0, \qquad (28a)$$

where μ_F and μ_{Xe} are the reciprocal masses of the fluorine and xenon atoms, respectively. The elements of the matrix L^{-1} were found to be:

$$Q_1 = 0.5618\times10^{-11} S(A_{1g}),$$
$$Q_2 = 0.6061\times10^{-19} S(A_{2u}),$$
$$Q_3 = 0.5391\times10^{-19} S(B_{1g}),$$
$$Q_4 = 0.7622\times10^{-19} S(B_{1u}),$$
$$Q_5 = 0.5618\times10^{-11} S(B_{2g}),$$
$$Q_6 = 0.4585\times10^{-11} S(E_u)_R - 0.2311\times10^{-19} S(E_u)_\gamma,$$
$$Q_7 = 0.0134\times10^{-11} S(E_u)_R + 0.6643\times10^{-19} S(E_u)_\gamma. \qquad (28b)$$

Table VI lists the values of $(\partial \mathbf{r}/\partial q_a)_0$ for the normal vibrations. Also given in Table VI are the values of $\langle Q_a^2\rangle^{\frac{1}{2}}$ calculated from Eq. (14). By a transformation of coordinates the xenon atom was considered fixed and the resulting vibration dipole on each fluorine atom was calculated. Equation (13) with Z_σ equal to unity gives

$$a_{2u},\ \mu_F = 0.0643\ ea_0 \text{ (in } z \text{ direction)},$$
$$b_{1u},\ \mu_F = 0.0586\ ea_0 \text{ (in } z \text{ direction)},$$

where a_0 is the Bohr radius.

TABLE IV. **B** matrix for XeF_4.

	Xe			F_1			F_2			F_3			F_4		
	x	y	z	x	y	z	x	y	z	x	y	z	x	y	z
$S(A_{1g})$	0	0	0	−0.500	0	0	0	0.500	0	0.500	0	0	0	−0.500	0
$S(A_{2u})$	0	0	1.473 ×10⁸	0	0	−3.683 ×10⁷	0	0	−3.683 ×10⁷	0	0	−3.683 ×10⁷	0	0	−3.683 ×10⁷
$S(B_{1g})$	0	0	0	0	−5.208 ×10⁷	0	5.208 ×10⁷	0	0	0	5.208 ×10⁷	0	−5.208 ×10⁷	0	0
$S(B_{1u})$	0	0	0	0	0	3.683 ×10⁷	0	0	−3.683 ×10⁷	0	0	3.683 ×10⁷	0	0	−3.683 ×10⁷
$S(B_{2g})$	0	0	0	−0.500	0	0	0	−0.500	0	0.500	0	0	0	0.500	0
$S(E_u)_R$	1.00	0	0	−0.500	0	0	0	−0.500	0	−0.500	0	0	0	−0.500	0
$S(E_u)_\gamma$	5.208 ×10⁷	0	0	0	−3.683 ×10⁷	0	−3.683 ×10⁷	0	0	0	−3.683 ×10⁷	0	−3.683 ×10⁷	0	0

TABLE V. Potential-energy matrix for XeF_4.

$S(A_{1g})$	$S(A_{2u})$	$S(B_{1g})$	$S(B_{1u})$	$S(B_{2g})$	$S(E_u)_R$	$S(E_u)_\gamma$
$F_R+2F_R'+F_R''$	0	0	0	0	0	0
	$F_\beta+F_\beta'$	0	0	0	0	0
		$F_\gamma-2F_\gamma'+F_\gamma''$	0	0	0	0
			$F_\beta-F_\beta'$	0	0	0
				$F_R-2F_R'+F_R''$	0	0
					F_R-F_R''	$\sqrt{2}(F_{R\gamma}-F_{R\gamma}')$
						$F_\gamma-F_\gamma''$

As in the case of XeF_2 these dipoles were considered to interact with a charge density on the stationary xenon atom. Note that $\psi(a_{2u})$ has no xenon s character. Therefore, upon expanding the molecular orbitals, only the charge density $e\psi(a_{1g})\psi(a_{2u})$ will have terms transforming like dipoles since of all the relevant molecular orbitals only that of a_{1g} symmetry has a xenon $5s$ component. The importance of the charge densities corresponding to mixing the molecular orbitals b_{1g}, a_{2g}, b_{2g} or e_g with a_{2u} will be much smaller since they involve contributions transforming as quadrupoles and overlap type terms; these contributions will therefore be neglected. The two e_u normal modes of vibration are therefore much less important and in this approximation do not enter into the calculation. For the a_{2u} vibration $\nu=291$ cm^{-1} and for the b_{1u} vibration $\nu=221$ cm^{-1}.[14] $\psi(a_{1g})$ was represented in the form

$$\psi(a_{1g}) = (a/2)[\phi(2p_xF_1)+\phi(2p_xF_2)+\phi(2p_xF_3)+\phi(2p_xF_4)] + (b/2)[\phi(2sF_1)+\phi(2sF_2)+\phi(2sF_3)+\phi(2sF_4)] + c\phi(5s\mathrm{Xe}). \quad (29)$$

The secular equation was solved as described above to give: $a=-0.596$, $b=-0.260$, and $c=0.593$. $\psi(a_{2u})$ was represented in the form

$$\psi(a_{2u}) = (a/2)[\phi(2p_zF_1)+\phi(2p_zF_2)+\phi(2p_zF_3)+\phi(2p_zF_4)] + b\phi(5p_z\mathrm{Xe}). \quad (30)$$

Solution of the secular equation gives: $a=-0.293$ and $b=0.925$. Expanding the molecular orbitals in terms of atomic orbitals, as in the case of XeF_2, leads to

$$\psi(a_{1g})\psi(a_{2u}) = 0.5485\phi(5s\mathrm{Xe})\phi(5p_z\mathrm{Xe}). \quad (31)$$

This charge distribution was replaced by a point dipole of the same magnitude (calculated to be 0.689 ea_0 in the z direction). Remembering that four fluorine atoms interact with the xenon charge distribution, the calculated interaction energy contributions from the two normal vibrations are

$$(W_{ks})a_{2u}=0.1048 \text{ eV},$$
$$(W_{ks})b_{1u}=0.0957 \text{ eV}. \quad (32)$$

Equation (10) is used together with the following empirical data from Ref. 3:

$$E(E_g\leftarrow A_{1g})=5.4-4.8 \text{ eV},$$
$$E(E_u\leftarrow A_{1g})=9.36 \text{ eV},$$
$$f(E_u\leftarrow A_{1g})=0.80, \quad (33)$$

TABLE VI. Values of $(\partial r/\partial q_a)_0$ and $\langle Q^2\rangle^{\frac{1}{2}}$ for XeF_4.[a]

		A_{1g}	A_{2u}	B_{1g}	B_{1u}	B_{2g}	$E_{u(R)}$	$E_{u(\gamma)}$
	x	−0.1148	0	0	0	−0.1148	−0.0937	0.0027
F_1	y	0	0	−0.1147	0	0	−0.0348	−0.1000
	z	0	−0.0912	0	+0.1147	0	0	0
	x	0	0	0.1147	0	0	−0.0348	−0.1000
F_2	y	0.1148	0	0	0	−0.1148	−0.0937	0.0027
	z	0	−0.0912	0	−0.1147	0	0	0
	x	0.1148	0	0	0	+0.1148	−0.0937	0.0027
F_3	y	0	0	0.1147	0	0	−0.0348	−0.1000
	z	0	−0.0912	0	+0.1147	0	0	0
	x	0	0	−0.1147	0	0	−0.0348	−0.1000
F_4	y	−0.1148	0	0	0	+0.1148	−0.0937	0.0027
	z	0	−0.0912	0	−0.1147	0	0	0
	x	0	0	0	0	0	0.0345	0.0198
Xe	y	0	0	0	0	0	0	0
	z	0	0.0532	0	0	0	0	0
$\langle Q^2\rangle^{\frac{1}{2}}$		0.1762	0.2406	0.2676	0.2761	0.1832	0.1696	0.3702

[a] Values of $(\partial r/\partial q_a)_0$ are multipled by $N^{-\frac{1}{2}}$ where N is Avogadro's number. Values of $\langle Q^2\rangle^{\frac{1}{2}}$ are multipled by $N^{\frac{1}{2}}$.

so that at $T=303°K$,

$$f(E_g \leftarrow A_{1g})\,(\text{est}) = 0.001. \tag{34}$$

V. SPIN-ORBIT COUPLING

The study of spin forbidden (i.e., singlet–triplet) transitions in the xenon fluorides is of considerable interest both for the description of the excited states of these molecules and for the insight it provides into the intermolecular heavy atom enhancement effect.[15] The latter phenomenon is of interest in the study of the triplet states of aromatic molecules. In the quantum-mechanical treatment of atomic structure both the diagonal and nondiagonal matrix elements of the spin–orbit interaction are of the same order of magnitude, being determined by the spin–orbit coupling parameter

$$\xi = \frac{e\hbar^2}{2m^2c^2}\int R(r)\left(r^{-1}\frac{\partial V}{\partial r}\right)R(r)\,r^2dr, \tag{35}$$

where $R(r)$ is the radial wavefunction and V the potential. The parameter ξ is determined from the experimental multiplet splittings in atomic spectra. Oscillator strengths and lifetimes of excited states can be accurately reproduced[16] by introduction of an additional parameter which takes into account the difference between the radial wavefunctions in the singlet and triplet states. The theoretical treatment of singlet–triplet transitions in polyatomic molecules originated with the work of McClure[17] and has been continued by several other workers.[18–20] In the present treatment of intercombination probabilities in the molecular spectra of the xenon fluorides we shall attempt to reduce the spin–orbit coupling matrix elements to one center terms which can then be approximated by appropriate parameters derived from atomic spectra. This semiempirical treatment is advantageous in view of the lack of knowledge of the appropriate SCF atomic orbitals for the Xe atom. An *a priori* computation of the molecular spin orbital coupling parameters is not feasible at the present time.

It is well known that in molecules characterized by a singlet ground state the perturbation resulting from spin–orbit coupling leads to mixing of the triplet excited state with some singlet states and thereby to a finite transition probability from the ground state to the excited triplet state. In the approximation employed in this work the molecular spin–orbit coupling operator is given by

$$H_s = (e\hbar/4m^2c^2)\sum_i \mathfrak{d}(i)\cdot\mathbf{p}(i)\times\nabla_i V, \tag{36}$$

where $\mathfrak{d}(i)$ is the Pauli spin operator, $\mathbf{p}$ the linear momentum, ∇_i the gradient operator, and V the potential due to all the nuclei and all the other electrons. The sum is taken over all the electrons. The interaction between the spin of one electron and the orbital motion of the others is neglected, so that the spin–orbit coupling Hamiltonian, H_s, can be displayed in the form of a sum of one electron operators. Introducing a system of Cartesian coordinates, H_s is given by

$$H_s = \frac{ie\hbar^2}{4m^2c^2}\sum_i[\sigma_x(i)\,a_x(i)+\sigma_y(i)\,a_y(i)+\sigma_z(i)\,a_z(i)], \tag{37}$$

where the operators a_x, a_y and a_z are:

$$a_x(i) = \frac{\partial V}{\partial y_i}\frac{\partial}{\partial z_i} - \frac{\partial V}{\partial z_i}\frac{\partial}{\partial y_i},$$

$$a_y(i) = \frac{\partial V}{\partial z_i}\frac{\partial}{\partial x_i} - \frac{\partial V}{\partial x_i}\frac{\partial}{\partial z_i},$$

$$a_z(i) = \frac{\partial V}{\partial x_i}\frac{\partial}{\partial y_i} - \frac{\partial V}{\partial y_i}\frac{\partial}{\partial x_i}. \tag{38}$$

When the eigenfunctions of the spin independent Hamiltonian are employed as zero-order wavefunctions, the matrix elements of H_s between the triplet wavefunction Ψ_T and a singlet wavefunction Ψ_S will vanish unless the two configurations differ only in the spin of one electron, and in the occupancy number of a single molecular orbital. In addition, a symmetry restriction is imposed: the direct product $\Psi_T\times\Psi_S$ must belong to the same irreducible representation of the molecular point group as one of the spatial components a_x, a_y or a_z of the operator H_s. As a_z, a_y and a_z transform like the rotation operators R_x, R_y and R_z, respectively, at least one of the three direct products $R_x\times\Psi_T\times\Psi_S$, $R_y\times\Psi_T\times\Psi_S$, or $R_z\times\Psi_T\times\Psi_S$ must contain the A_{1g} representation.

The Hermitian matrices for the components of $\sigma(1)$ and $\sigma(2)$ for a basis set consisting of two electron spin

TABLE VII. Spin-orbit coupling in XeF_2 ($D_{\infty h}$ symmetry).

Triplet state	Singlet state	Mixing operators	Contribution to f
$^3A_{2u}(a_{1g}\rightarrow a_{2u})$	$^1E_{1u}(e_{1g}\rightarrow a_{2u})$	a_z, a_y	$\sim10^{-5}$
	$^1E_{1u}[e_{1u}\rightarrow a_{1g}(\text{Xe}6s)]$	a_z, a_y	0
	$^1E_{1u}[a_{1g}\rightarrow e_{1u}(\text{Xe}6p)]$	a_z, a_y	$\sim10^{-6}$
	$^1A_{1u}[e_{1u}\rightarrow e_{1g}(\text{Xe}5d)]$	a_x	0
	$^1E_{1u}[e_{1u}\rightarrow e_{2g}(\text{Xe}5d)]$	a_z, a_y	0
$^3E_{1u}(e_{1g}\rightarrow a_{2u})$	$^1E_{1u}$	a_x	$\sim10^{-6}$
	$^1A_{2u}(a_{1g}\rightarrow a_{2u})$	a_z, a_y	$\sim10^{-4}$

[15] S. P. McGlynn, R. Sunseri, and N. Christodouleas, J. Chem. Phys. **37**, 1818 (1962).
[16] G. W. King and J. H. Van Vleck, Phys. Rev. **56**, 464 (1937).
[17] D. S. McClure, J. Chem. Phys. **20**, 682 (1952).
[18] M. Mizushima and S. Koide, J. Chem. Phys. **20**, 765 (1952).
[19] J. W. Sidman, J. Chem. Phys. **29**, 644 (1958).
[20] H. F. Hameka and L. J. Oosterhoff, Mol. Phys. **1**, 358 (1958).

eigenfunctions are given by

	$\sigma_x(1)$				$\sigma_y(1)$				$\sigma_z(1)$			
$\psi_1=[\alpha(1)\beta(2)+\alpha(2)\beta(1)]/\sqrt{2}$	0	$1/\sqrt{2}$	$1/\sqrt{2}$	0	0	$i/\sqrt{2}$	$-i/\sqrt{2}$	0	0	0	0	1
$\psi_2=\alpha(1)\alpha(2)$	$1/\sqrt{2}$	0	0	$-1/\sqrt{2}$	$-i/\sqrt{2}$	0	0	$i/\sqrt{2}$	0	1	0	0
$\psi_3=\beta(1)\beta(2)$	$1/\sqrt{2}$	0	0	$1/\sqrt{2}$	$i/\sqrt{2}$	0	0	$i/\sqrt{2}$	0	0	-1	0
$\psi_4=[\alpha(1)\beta(2)-\alpha(2)\beta(1)]/\sqrt{2}$	0	$-1/\sqrt{2}$	$1/\sqrt{2}$	0	0	$-i/\sqrt{2}$	$-i/\sqrt{2}$	0	1	0	0	0
	$\sigma_x(2)$				$\sigma_y(2)$				$\sigma_z(2)$			
$\psi_1=[\alpha(1)\beta(2)+\alpha(2)\beta(1)]/\sqrt{2}$	0	$1/\sqrt{2}$	$1/\sqrt{2}$	0	0	$i/\sqrt{2}$	$-i/\sqrt{2}$	0	0	0	0	-1
$\psi_2=\alpha(1)\alpha(2)$	$1/\sqrt{2}$	0	0	$1/\sqrt{2}$	$-i/\sqrt{2}$	0	0	$-i/\sqrt{2}$	0	1	0	0
$\psi_3=\beta(1)\beta(2)$	$1/\sqrt{2}$	0	0	$-1/\sqrt{2}$	$i/\sqrt{2}$	0	0	$-i/\sqrt{2}$	0	0	-1	0
$\psi_4=[\alpha(1)\beta(2)-\alpha(2)\beta(1)]/\sqrt{2}$	0	$1/\sqrt{2}$	$-1/\sqrt{2}$	0	0	$i/\sqrt{2}$	$i/\sqrt{2}$	0	-1	0	0	0.

(39)

Hence, the singlet function is mixed with the $M_s=0$ component of the triplet function by $\sigma_z(i)$ and with the $M_s=\pm 1$ triplet components by $\sigma_x(i)$ and by $\sigma_y(i)$. Carrying out the summation over the electronic spin coordinates and applying the molecular orbital approximation, the molecular spin–orbit coupling matrix elements are reduced to one-electron integrals.

When the separations between the triplet state and the perturbing singlet states are large compared with the off diagonal matrix elements of H_s, the application of perturbation theory is legitimate and the oscillator strength for the spin-forbidden transition is given by

$$f_{G\to T}=\sum_S f_{G\to S}\frac{E_{G\to T}}{E_{G\to S}}\frac{|\langle\Psi_T|H_S|\Psi_S\rangle|^2}{(E_{G\to S}-E_{G\to T})^2}, \qquad (40)$$

where

$$|\langle\Psi_T|H_S|\Psi_S\rangle|^2=(e\hbar^2/4m^2c^2)^2(|\langle\psi_a|a_x|\psi_b\rangle|^2 + |\langle\psi_a|a_y|\psi_b\rangle|^2+|\langle\psi_a|a_z|\psi_b\rangle|^2). \qquad (41)$$

ψ_a and ψ_b are the unmatched molecular orbitals in Ψ_T and Ψ_S and G, T, and S refer to the ground, triplet, and singlet states, respectively. When $|\langle\Psi_T|H_S|\Psi_S\rangle|$ is of the same order of magnitude as $E_{G\to S}-E_{G\to T}$ an intermediate coupling scheme has to be employed.

In our treatment the spin–orbit perturbation of the ground singlet state by excited triplets will not be considered.[21] For the xenon fluorides this mixing is expected to be small.

VI. SINGLET–TRIPLET TRANSITIONS IN XeF_2

The perturbation treatment will now be used to obtain an order of magnitude estimate of the singlet–triplet transition probability in XeF_2. In the symmetry group $D_{\infty h}$ of the linear triatomic molecule (Fig. 3) a_z and a_y transform like E_{1g} while a_x transforms like A_{2g}. The lowest triplet state of the molecule is expected to be a $^3A_{2u}$ state corresponding to the $a_{1g}\to a_{2u}$ transition. The $^3A_{2u}$ state can be mixed with $^1E_{1u}$ states by a_z and a_y and with $^1A_{1u}$ type states by a_x. It is interesting to note that the mixing of $^3A_{2u}$ with the corresponding $^1A_{2u}$ state is symmetry forbidden and no intensity borrowing can occur from the strong 1580-Å band of XeF_2. Other singlet excited states which can be mixed with the $^3A_{2u}$ state are listed in Table VII. We consider states arising from excitation to orbitals mainly involving the Xe atom orbitals, as these are expected to lead to the greatest effect.

The mixing of the $^3A_{2u}$ state with the singlet Rydberg-type excited states $e_{1u}\to a_{1g}$, $e_{1u}\to e_{1g}$, and $e_{1u}\to e_{2g}$ is negligible since the singlet and triplet states differ by the occupation of two orbitals. The Rydberg state $^1E_{1u}$ arising from the excitation $a_{1g}\to e_{1u}$ (Xe6p) was not experimentally observed up to 13 eV and the corresponding excitation energy is expected to be about 15 eV. The oscillator strength for this singlet–singlet $\sigma\to\pi^*$-type transition is expected to be low (probably of the order of 10^{-1} to 10^{-2}). The spin–orbit coupling matrix element can be estimated by considering only one-center terms. The two unmatched orbitals in these two excited states are the a_{2u} and the e_{1u} (Xe6p) orbitals, so that the one-center terms are of the order of

$$(ie\hbar^2/4m^2c^2)[\langle\phi(6p_y\,\mathrm{Xe})|a_z|\phi(5p_x\,\mathrm{Xe})\rangle + \langle\phi(6p_z\,\mathrm{Xe})|a_y|\phi(5p_x\,\mathrm{Xe})\rangle].$$

The absolute value of this matrix element is expected to lie between $\xi_{Xe}(5p)/2=0.37$ eV[22] and $\xi_{Xe}(6p)/2=0.33$ eV.[22] A reasonable order of magnitude estimate

[21] L. Goodman and V. G. Krishna, J. Chem. Phys. **37**, 2721 (1962).

[22] C. E. Moore, Natl. Bur. Std. (U.S.) Circ. No. 469 (1949).

will be 0.1 to 0.2 eV. Hence, the transition strength to the $^3A_{2u}$ state due to the intensity borrowing from the E_{1u} (Xe6p) state is expected to be of the order of 10^{-6}.

Consider now the intensity borrowing from the $^1E_{1u}$ state (due to the $e_{1g}\rightarrow a_{2u}$ excitation). The spin–orbit coupling parameter for this mixing can be displayed in the form:

$$\langle\psi(a_{1g})\mid H_s\mid\psi(e_{1g})\rangle=\langle(1/\sqrt{2})[\phi(2p_z\,F_3)-\phi(2p_z\,F_2)]\mid H_s\mid(1/\sqrt{2})[\phi(2p_x\,F_3)-\phi(2p_x\,F_2)]\rangle$$

$$\approx(ie\hbar^2/4m^2c^2)[\langle\phi(2p_x\,F_2)\mid a_z\mid\phi(2p_y\,F_2)\rangle+\langle\phi(2p_x\,F_2)\mid a_y\mid\phi(2p_z\,F_2)\rangle]. \quad (42)$$

These terms involve only the contribution of the fluorine atom, and each of the one center terms can be approximated by $\xi_F(2p)/2=135$ cm^{-1}.[22] The intensity of the singlet–singlet $\pi\rightarrow\sigma^*$ type transition is expected to be low. It has not been observed experimentally[1] and is probably masked by the transition to the $^1A_{2u}$ state. A reasonable estimate for the oscillator strength for this singlet–singlet transition is $\sim$0.01. Taking the energy difference between the triplet and singlet state as 2 eV, its contribution to the transition strength of the $^1A_{1g}\rightarrow{}^3A_{2u}$ transition is only $\sim10^{-7}$. Our estimate of the contribution does not include the mixing of the Xe4d orbitals in the a_{1g} and e_{1u} molecular orbitals, but this mixing has been shown to be small.[23] A rough estimate indicates that a 10% admixture of d character leads to a contribution of 10^{-6} to the oscillator strength for the $^1A_{1g}\rightarrow{}^3A_{2u}$ transition.

Another singlet–triplet absorption in XeF_2 which should be considered is the $^1A_{1g}\rightarrow{}^3E_{1u}$ transition arising from the excitation $e_{1g}\rightarrow a_{2u}$. Mixing with the $^1A_{2u}$ state is possible; the spin–orbit coupling matrix element is again given by Eq. (42). Using the experimental spectroscopic data for the $^1A_{1g}\rightarrow{}^1A_{2u}$ ($f=0.45$) transition and assuming that the energy separation between the singlet and triplet states is $\sim$2 eV, the expected intensity borrowing will be of the order of 10^{-4}. It should be noted that the $^3E_{1u}$ state can interact with the corresponding $^1E_{1u}$ state. The problem of spin–orbit coupling in orbitally degenerate states will be treated in detail in the next section, and we do not here reproduce in detail the computation for XeF_2. It is found that the spin–orbit coupling parameter is again determined by the F atom spin–orbit coupling, and the transition strength due to intensity borrowing is of the order of 10^{-6} to 10^{-7}.

We conclude that the singlet–triplet transitions in XeF_2, i.e., $^1A_{1g}\rightarrow{}^3A_{2u}$ and $^1A_{1g}\rightarrow{}^3E_{1u}$, should be characterized by a relatively low oscillator strength $f\lesssim10^{-4}$. This is a surprising conclusion since it indicates that in spite of the presence of the heavy atom, the symmetry restrictions imposed and the lack of nearby excited states leads to a low singlet–triplet transition probability.

[23] L. L. Lohr and W. N. Lipscomb, *Noble Gas Compound* (University of Chicago Press, Chicago, Illinois, 1963), p. 347.

VII. INTERMEDIATE COUPLING SCHEME FOR XeF_4

The first triplet state in XeF_4 is expected to be a ^3E_u state arising from the transition $b_{1g}\rightarrow e_u$[24] (see Fig. 4). Consider the symmetry properties of the operators a_x, a_y, and a_z for this molecule. In the symmetry group D_{4h}, a_x, and a_y transform like e_g while a_z transforms like b_{2g}. Hence a ^3E_u state can be spin–orbit coupled with $^1A_{1u}$, $^1A_{2u}$, $^1B_{1u}$, and $^1B_{2u}$ states by a_x and a_y and with ^1E_u states by a_z.

The spin and symmetry allowed transitions in XeF_4 have been studied previously[3] and are found to be: (1) $b_{1g}\rightarrow e_u$; (2) $a_{2g}\rightarrow e_u$; (3) $e_g\rightarrow e_u$; (4) $b_{2g}\rightarrow e_u$; (5) $a_{1g}\rightarrow e_u$. (see Fig. 4). The transitions (1), (2), (4), and (5) are $^1A_{1g}\rightarrow{}^1E_u$, while transition (3) is $^1A_{1g}\rightarrow{}^1A_{1u}+{}^1A_{2u}+{}^1B_{1u}+{}^1B_{2u}$. Hence, all these singlet excited states can mix with the ^3E_u state. It is important to notice that in the case of XeF_4 the doubly degenerate triplet state mixes with the corresponding singlet via spin–orbit interaction. As a first approximation configuration interaction can now be disregarded and only the mixing of the ^3E_u and ^1E_u excited states arising from the same configuration. The energy separation between these two pure spin states may be rather small (of the order of 1 to 2 eV) so that the perturbation treatment used in Secs. V and VI seems inappropriate and a variational method will be used. The problem will be treated in the intermediate coupling scheme, formally similar to that used for the p^5s states of rare-gas atoms[25] and ps configurations of some impurity centers in ionic crystals[26] and for excited states of halide crystals.[27]

The Hamiltonian for the system is taken to be

$$H=H^0+H_s \quad (43)$$

and the wavefunction for the excited states is expressed in terms of the singlet and triplet wavefunction

$$\Psi=a[\Psi(^1E_u{}^x)+\Psi(^1E_u{}^y)]+\sum_{i=1}^{3}b_i[\Psi_i(^3E_u{}^x)+\Psi_i(^3E_u{}^y)], \quad (44)$$

[24] Another possible assignment is the $\pi\rightarrow\sigma^*$ transition $a_{2g}\rightarrow e_u$ ($^1A_{1g}\rightarrow{}^3E_u$). We reach the same general conclusions for both transitions.

[25] R. S. Knox, Phys. Rev. **110**, 375 (1958).

[26] F. E. Williams, B. Segall, and P. D. Johnson, Phys. Rev. **108**, 46 (1961).

[27] R. S. Knox and N. Inchauspe, Phys. Rev. **116**, 1093 (1959).

where the three triplet states are labeled as in Eq. (39). The subscripts x and y refer to the spatial direction of the e_u orbitals [see Fig. 3(b)]. The secular matrix takes the form

$$\begin{pmatrix} \mathbf{A} & & \mathbf{O} \\ & \mathbf{A}^+ & \\ & & \mathbf{B} \\ \mathbf{O} & & \\ & & \mathbf{B}^+ \end{pmatrix}$$

with

$$\mathbf{A}=\begin{array}{c|cc} & {}^1E^x & {}^3E_1^y \\ \hline {}^1E^x & E^0+2G & Z \\ {}^3E_1^y & Z^* & E^0 \end{array}, \qquad \mathbf{B}=\begin{array}{c|cc} & {}^3E_2^x & {}^3E_2^y \\ \hline {}^3E_2^x & E^0 & Z \\ {}^3E_2^y & Z^* & E^0 \end{array},$$

$$\mathbf{A}^+=\begin{array}{c|cc} & {}^1E^y & {}^3E_1^x \\ \hline {}^1E^y & E^0+2G & Z^* \\ {}^3E_1^x & Z & E^0 \end{array}, \qquad \mathbf{B}^+=\begin{array}{c|cc} & {}^3E_3^x & {}^3E_3^y \\ \hline {}^3E_3^x & E^0 & Z^* \\ {}^3E_3^y & Z & E^0 \end{array}.$$

Here E^0 is the energy of the pure spin triplet states:

$$E^0=\langle\Psi_i({}^3E_u^x)\mid H^0\mid\Psi_i({}^3E_u^x)\rangle = \langle\Psi_i({}^3E_u^y)\mid H^0\mid\Psi_i({}^3E_u^y)\rangle \qquad i=1,2,3. \quad (45)$$

The energy difference between the pure spin singlet and triplet states is given by $2G$, where G is the exchange integral between the two unmatched orbitals in the ground and excited states

$$E^0+2G=\langle\psi({}^1E_u^x)\mid H^0\mid\psi({}^1E_u^x)\rangle = \langle\psi({}^1E_u^y)\mid H^0\mid\psi({}^1E_u^y)\rangle. \quad (46)$$

The nonvanishing off-diagonal matrix elements are

$$Z=\langle\Psi({}^1E_u^x)\mid H_s\mid\Psi_1({}^3E_u^y)\rangle = \langle\Psi_1({}^3E_u^x)\mid H_s\mid\Psi({}^1E_u^y)\rangle = \langle\Psi_2({}^3E_u^x)\mid H_s\mid\Psi_2({}^3E_u^y)\rangle = \langle\Psi_3({}^3E_u^x)\mid H_s\mid\Psi_3({}^3E_u^y)\rangle. \quad (47)$$

It should be noted that the diagonal spin–orbit matrix elements

$$\langle\Psi({}^1E_u^{x,y})\mid H_s\mid\Psi({}^1E_u^{x,y})\rangle$$

and

$$\langle\Psi_1({}^3E_u^{x,y})\mid H_s\mid\Psi_1({}^3E_u^{x,y})\rangle$$

vanish due to spin orthogonality while the matrix elements

$$\langle\Psi_2({}^3E_u^{x,y})\mid H_s\mid\Psi_2({}^3E_u^{x,y})\rangle$$

and

$$\langle\Psi_3({}^3E_u^{x,y})\mid H_s\mid\Psi_3({}^3E_u^{x,y})\rangle$$

vanish because of the symmetry restrictions imposed (H_s involves only the $a_z\sigma_z$ operator).

It is at once apparent that only the triplet component $\Psi_1({}^3E_u)$ mixes with the singlet $\Psi({}^1E_u)$ and hence in this approximation optical transitions to only this triplet state are expected. It is clear then that we are only interested in the wavefunction

$$\Psi_\pm=a_\pm\Psi({}^1E_u^x)+b_\pm\Psi_1({}^3E_u^y). \quad (48)$$

The coefficients $a_\pm$ and $b_\pm$ are readily obtained from the secular equation

$$(E^0+2G-E)a_\pm+Zb_\pm=0, \qquad Z^*a_\pm+(E^0-E)b_\pm=0. \quad (49)$$

The energies are

$$E_\pm=E^0+G\pm(G^2+\mid Z\mid^2)^{\frac{1}{2}} \quad (50)$$

and the energy splitting between the two states is

$$\delta=E_+-E_-=2(G^2+\mid Z\mid^2)^{\frac{1}{2}}. \quad (51)$$

The ratio of the transition probabilities involved in the two transitions is

$$\frac{f_+}{f_-}=\frac{h\nu_+}{h\nu_-}\frac{\mid a_+\mid^2}{\mid a_-\mid^2}; \quad (52)$$

here $h\nu_\pm$ are the energies involved in the two transitions. The ratio

$$\rho=\mid a_+\mid^2/\mid a_-\mid^2 \quad (53)$$

is readily obtained from the solution of the secular Eq. (49) by imposition of the normalization condition on the wavefunction in Eq. (48). We are thereby led to the result

$$\rho=\frac{(E^0+2G-E_-)^2+\mid Z\mid^2}{(E^0+2G-E_+)^2+\mid Z\mid^2}. \quad (54)$$

Let $x=G/\mid Z\mid$, whereupon

$$\rho=\frac{1+x^2+x(1+x^2)^{\frac{1}{2}}}{1+x^2-x(1+x^2)^{\frac{1}{2}}}=1+2x^2+2x(1+x^2)^{\frac{1}{2}}. \quad (55)$$

The oscillator strength ratio is thus found to be determined by the ratio of the exchange integral and the spin–orbit coupling matrix element. For the limiting case of extremely strong spin–orbit coupling $x\to 0$ and $\rho\to 1$. When spin–orbit coupling is weak, i.e., $x\gg 1$, then $\rho=4x^2$.

The present treatment differs from the intermediate coupling scheme for the atomic case in that the diagonal spin–orbit matrix element for the pure spin–triplet states vanishes (due to the lower symmetry of the molecular systems).

In order to obtain an estimate for the singlet–triplet oscillator strength ratio in XeF_4, the matrix elements G and Z must be evaluated. The spin–orbit coupling

matrix element Z can be displayed in the form

$$Z=\langle\Psi(^1E_u^x)\mid H_s\mid\Psi_1(^3E_u^y)\rangle$$
$$=\langle\psi(e_u^x)_1\mid a_z(1)\mid\psi(e_u^y)_1\rangle, \quad (56)$$

while the e_u molecular orbitals in XeF_4 can be represented by

$$\psi(e_u)=\alpha\begin{Bmatrix}\phi(5p_x\,\mathrm{Xe})\\ \phi(5p_y\,\mathrm{Xe})\end{Bmatrix}+\beta\begin{Bmatrix}\phi(2p_x\,\mathrm{F_1})+\phi(2p_x\,\mathrm{F_3})\\ \phi(2p_x\,\mathrm{F_2})+\phi(2p_x\,\mathrm{F_4})\end{Bmatrix}, \quad (57)$$

where $\alpha=0.991$ and $\beta=-0.210$.

In the calculation of Z only one-center terms are considered and the contribution of the F atoms is neglected ($\beta^2\ll1$ and $\xi_F\ll\xi_{Xe}$).

Since $\alpha^2\approx1$, we set

$$Z=\langle\phi(5p_x\,\mathrm{Xe})\mid a_z\mid\phi(5p_y\,\mathrm{Xe})\rangle. \quad (58)$$

Now, from Eq. (38) it readily follows that

$$Z=[ie\hbar^2/(2mc)^2]$$
$$\times\left\langle\phi(5p_x\,\mathrm{Xe})\left|\frac{\partial V}{\partial x}\frac{\partial}{\partial y}-\frac{\partial V}{\partial y}\frac{\partial}{\partial x}\right|\phi(5p_y\,\mathrm{Xe})\right\rangle. \quad (59)$$

Representing the Xe$5p_x$ and Xe$5p_y$ atomic orbitals in terms of spherical harmonics,

$$\phi(5p_x\,\mathrm{Xe})=(1/\sqrt{2})\,R_{\mathrm{Xe}^{5p}}(r)[y_{11}(\theta,\phi)+y_{1-1}(\theta,\phi)]$$
$$\phi(5p_y\,\mathrm{Xe})=(1/\sqrt{2}i)\,R_{\mathrm{Xe}^{5p}}(r)[y_{11}(\theta,\phi)-y_{1-1}(\theta,\phi)], \quad (60)$$

it is found that

$$Z=\frac{ie\hbar^2}{(2mc)^2}\left\langle R_{\mathrm{Xe}^{5p}}(r)\left|r^{-1}\frac{\partial V}{\partial r}\right|R_{\mathrm{Xe}^{5p}}(r)\right\rangle. \quad (61)$$

By comparing this result with Eq. (35) we may express Z in terms of the spin–orbit coupling constant for the Xe atom

$$Z=i\xi_{\mathrm{Xe}}(5p)/2. \quad (62)$$

A detailed study of the Rydberg states of XeF_2 indicates that the Xe atomic spin–orbit coupling parameter does not differ by more than 20% from the atomic value, $\xi_{\mathrm{Xe}}(5p)=0.75$ eV.

The parameter x is, therefore, approximated by $x=2G/\xi_{\mathrm{Xe}}(5p)$. It will be instructive at this stage to make a tentative guess regarding the expected value for the oscillator strength ratio f_+/f_- in the XeF_4 molecule compared to the intensity ratio for the atomic Xe atom transitions $^1S\rightarrow{}^1P_1$ and $^1S\rightarrow{}^3P_1$ arising from the atomic configuration p^5s. The oscillator strengths for the two atomic transitions are of the same order of magnitude. The theoretical treatment of the atomic case is quite straightforward leading to an expression for f_+/f_- which is determined by the ratio of the exchange integral to $\xi_{\mathrm{Xe}}(5p)$. However, the exchange integral involved in the molecular case is expected to be much larger than in the atomic case, as the former will involve molecular orbitals constructed from atomic orbitals characterized by the same principle quantum number. Hence, the oscillator strength ratio f_+/f_- is expected to be larger in the molecular case. In other words, the triplet band intensity is expected to be considerably weaker in XeF_4 than in the above mentioned atomic transition. A reliable evaluation of the exchange integral G cannot at present be given mainly due to the lack of knowledge of the atomic wavefunctions of Xe. Using the molecular orbital scheme, the exchange integral for the transition $b_{1g}\rightarrow e_u$ is given by

$$G(b_{1g},e_u)=(A^2/2)\langle\phi(2p_x\,\mathrm{F_1})(1)\phi(5p_x\,\mathrm{Xe})(1)\mid r_{12}^{-1}\mid\phi(2p_x\,\mathrm{F_1})(2)\phi(5p_x\,\mathrm{Xe})(2)\rangle$$
$$+(A^2/2)\langle\phi(2p_y\,\mathrm{F_2})(1)\phi(5p_x\,\mathrm{Xe})(1)\mid r_{12}^{-1}\mid\phi(2p_y\,\mathrm{F_2})(2)\phi(5p_x\,\mathrm{Xe})(2)\rangle$$
$$+(a^2/4)[\langle\phi(2p_x\,\mathrm{F_1})(1)\phi(2p_x\,\mathrm{F_1})(1)\mid r_{12}^{-1}\mid\phi(2p_x\,\mathrm{F_1})(2)\phi(2p_x\,\mathrm{F_1})(2)\rangle$$
$$-\langle\phi(2p_x\,\mathrm{F_1})(1)\phi(2p_x\,\mathrm{F_1})(1)\mid r_{12}^{-1}\mid\phi(2p_x\,\mathrm{F_3})(2)\phi(2p_x\,\mathrm{F_3})(2)\rangle]$$
$$+(a^2/2)\langle\phi(2p_x\,\mathrm{F_1})(1)\phi(2p_y\,\mathrm{F_2})(1)\mid r_{12}^{-1}\mid\phi(2p_x\,\mathrm{F_1})(2)\phi(2p_y\,\mathrm{F_2})(2)\rangle, \quad (63)$$

where one- and two-center terms only were considered. The molecular orbital coefficients for the e_u orbital are $A=0.971$, $a=0.559$.[3] The one-center F atom integrals were estimated using the Pariser–Parr[28] approximation. Two-center exchange terms were evaluated using Slater wavefunctions applying a computer program supplied by the Laboratory of Molecular Structure of the University of Chicago. These calculations lead to $G=1.02$ eV. The f_+/f_- ratio is quite sensitive to the value of x, for $x=1$, $\rho=5.7$, for $x=2$, $\rho=18$ while for $x=3$, $\rho=36$. From the estimate of G we may conclude that $x\approx2$ so that intensity borrowing from the 1850 Å allowed transition ($f=0.22$)[3] leads to a theoretically estimated oscillator strength for the corresponding $^1A_{1g}\rightarrow{}^3E_u$ of $f=0.007$.

[28] R. Pariser, J. Chem. Phys. **21**, 568 (1953).

VIII. EXPERIMENTAL DETAILS

A. Experimental Transition Intensities

The ultraviolet absorption spectra of XeF_2 and XeF_4 have been reported earlier.[1–3] Curves *a* in Figs. 5 and 6 show the absorption spectra from 2000 to 3000 Å. The

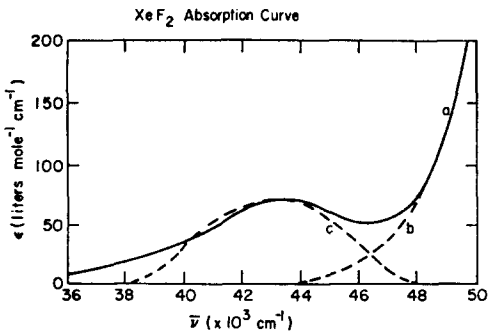

FIG. 5. The absorption spectrum of gaseous XeF_2 from 2000 to 3000 Å; Curves b and c represent the (Gaussian) components.

molar absorption coefficient was calculated using 3.8 mm as the vapor pressure of XeF_2 at 25°C[13] and 2.0 mm as the estimated vapor pressure of XeF_4 at 25°C. The sharply rising portion of each curve, corresponding to the onset of the $A_{1g}\rightarrow A_{2u}$ transition in XeF_2 and the $A_{1g}\rightarrow E_u$ transition in XeF_4 at 25°C, was fitted to a Gaussian function of the form

$$\epsilon=\epsilon_{max}\exp[-\sigma(\bar{\nu}-\bar{\nu}_0)^2]. \quad (64)$$

In Eq. (64), $\bar{\nu}_0$ corresponds to the wavenumber at the peak maximum, $\sigma^{\frac{1}{2}}$ is inversely related to the half-width of the peak, and ϵ_{max} is the molar absorption at the peak maximum. This calculated function is shown as curves *b* in Figs. 5 and 6. The remaining curve in XeF_2 was fitted to a Gaussian (Curve *c* in Fig. 6) and subtracted from the total intensity. The remainder of the absorption intensity was fitted to a Gaussian, Curve *d* in Fig. 6.

The parameters of the Gaussian analysis are given in Table VIII. The oscillator strength, when a function of the form in Eq. (64) is used, is given by

$$f=7.655\times10^{-9}\epsilon_{max}\sigma^{-\frac{1}{2}}. \quad (65)$$

From the Gaussian analysis and Eq. (65) we are led to the oscillator strengths listed in Table VIII. The σ values for the allowed transitions in XeF_2 and XeF_4 are in reasonable agreement with the half bandwidths previously determined.[3]

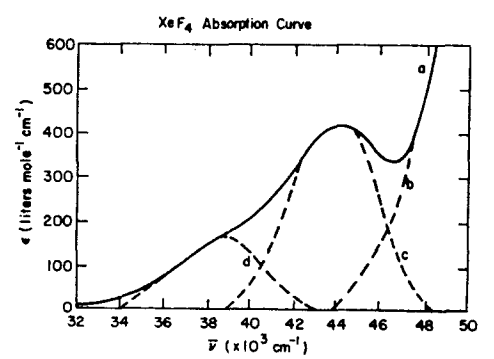

FIG. 6. The ultraviolet absorption spectrum of gaseous XeF_4; Curves b, c, and d represent the (Gaussian) components.

B. Temperature Dependence of the Intensity of the XeF_2 2330 Å Band

The theory of vibronic transitions makes a definite prediction concerning the temperature dependence of symmetry forbidden vibronically induced bands. As indicated by Eq. (10) each normal mode of the required symmetry contributes a term of the form $f_{0a}\coth(h\nu_a/2kT)$ with the coefficient f_{0a} determined from perturbation theory [Eq. (10)]. The temperature dependent factor arises from the integration over the Boltzmann distribution among the vibrational levels in the ground state.[7,10,11] The 2330 Å XeF_2 band seemed to be amenable for experimental investigation of the temperature dependence of the intensity of a vibronically induced band, as the π_u frequency in XeF_2 is low (213 cm^{-1}) so that a relatively large temperature effect in this band intensity is expected.

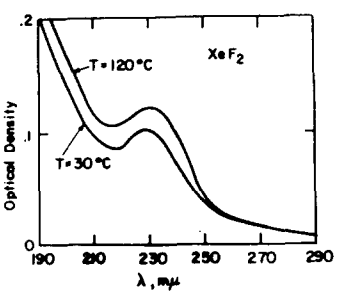

FIG. 7. The temperature dependence of the XeF_2 2330-Å band intensity.

An all quartz cell containing a pressure of XeF_2 equal to its room-temperature vapor pressure was enclosed in a solid copper block oven. The thermoregulated copper block was loaded into the water-cooled sample compartment of a Cary Model 14 Spectrophotometer. The heating element consisted of approximately 80 Ω of Nichrome wire wound on four insulated rods. The temperature control-indicator was a Fenwal Model 561 electronic indicating controller using a thermistor probe and capable of controlling to within 0.05°C. With the Model 14 Cary an auxiliary slide wire was used which had an indicating range of 0.0 to 0.2 units of optical density. The spectra obtained at 30° and 120°C are shown in Fig. 7.

A Gaussian analysis similar to that described above was carried out. The molar absorption coefficient at the peak maximum was 75 at 30°C and 83 at 120°C; the bandwidth parameter of Eq. (65), σ, was 0.88×10^{-7} cm^2 at both temperatures. The temperature induced increase in the oscillator strength is observed to be 0.12 ± 0.04%/deg in the region 30° to 120°C. That expected on the basis of Eq. (10) (taking $\nu_2=213$ cm^{-1} [13]) would be 0.3%/deg for XeF_2.

IX. DISCUSSION

The general scheme used for the analysis of the vibronically induced transitions in the xenon fluorides leads to the following conclusions:

(1) The oscillator strengths for the vibronically induced transitions in both XeF_2 and XeF_4 are about 10^{-3}.

(2) In XeF_2 the most important mixing of electronic states is caused by the π_u out of plane vibration, while in XeF_4 the a_{2u} and b_{1u} vibrations should be the most important. High resolution spectroscopy may be useful in confirming this conclusion, but possibly dissociation may mask all the vibrational structure.

(3) A relatively large temperature dependence of the XeF_2 vibronically induced band is expected.

At this point it will be useful to consider the approximations involved in the computation of the intensity of the symmetry forbidden transitions in the xenon fluorides.

(1) Only the vibronically induced mixing of excited states with energies up to 10 eV with the lowest excited state were considered; the mixing with Rydberg states in XeF_2 was not considered as these states are characterized by a relatively low transition probability. The mixing of excited states with the ground state in XeF_2 was also disregarded. However, the most important contributions to vibronic mixing have been included in the perturbation treatment.

(2) The effect of the core potential was neglected and complete screening of the nuclear charges by the other inner electrons was assumed.

(3) The transition charge density functions have been represented in the point dipole approximation.

(4) The molecular orbital scheme employed is based on the extended semiempirical Hückel scheme. However, 10% to 20% uncertainty in the LCAO coefficients will not appreciably alter our conclusions.

(5) The energies of excited states were taken from the experimental spectroscopic data.

Another important point which has to be considered is the possibility of configuration changes in the excited state. The $^1E_{1g}$ excited state of XeF_2 may be nonlinear. For the case of a linear molecule, the Jahn–Teller theorem is inapplicable to the degenerate $^1E_{1g}$ state, and detailed computations must be carried out to establish the most stable configuration. In the $^1E_{1g}$ state of the XeF_4 molecule, the Jahn–Teller theorem implies that the molecule will distort from the square planar configuration. The shape of the vibronically induced absorption bands (i.e., their vibrational details if these can be observed) will be affected by the nuclear framework distortions in the excited state. However, the limitations imposed by the Franck–Condon principle imply that the total vibronic band intensity has to be calculated in terms of the ground state nuclear configurations.

The following conclusions are reached regarding the spin forbidden transitions in the xenon fluorides:

TABLE VIII. Parameters from Gaussian analysis of spectra.

Band (Å)	ϵ_0 (liters/mole cm)	ν_0 (cm^{-1})	σ (cm^2)	f[a]
XeF_2				
1580	12 227	63 291	2.17×10^{-8}	0.64 (0.45)
2330	75	43 000	0.88×10^{-7}	0.002
XeF_4				
1840	4 800	54 349	5.52×10^{-8}	0.17 (0.22)
2280	398	43 750	1.20×10^{-7}	0.009
2580	160	38 750	1.34×10^{-7}	0.003

[a] The f values are calculated from the σ values derived from the profile analysis. The f values for the allowed transitions previously obtained[3] are given in parentheses.

(1) The transition probability for the $^1A_{1g}\rightarrow{}^3A_{2u}$ in XeF_2 is low ($f\leq10^{-5}$) because of symmetry restrictions. The transition probability for the $^1A_{1g}\rightarrow{}^3E_{1u}$ transition is relatively low ($f\leq10^{-4}$) as the spin–orbit coupling matrix element is determined by the fluorine atom spin–orbit coupling.

(2) In XeF_4 the intermediate coupling scheme predicts a relatively large transition probability to the first excited triplet ^3E_u states.

The theoretical estimates of the symmetry and spin forbidden transition strengths for the xenon fluorides will now be applied to the classification of the weak electronic transitions in XeF_2 and XeF_4.

The case of XeF_2 is fairly simple. Since only one weak band is experimentally observed with $f=0.002$ and since the expected singlet–triplet transitions are estimated to be extremely weak, the observed band is assigned to the vibronic transition $^1A_{1g}\rightarrow{}^1E_{1g}$. The calculated strength of the vibronic transition ($f=0.001$) agrees with this assignment and the temperature dependence study provides additional supporting evidence.

The locations of the singlet–triplet transitions $^1A_{1g}\rightarrow{}^3A_{2u}$ and $^1A_{1g}\rightarrow{}^3E_{1u}$ are not known. These may be hidden under the low-energy tail of the 1580 Å band[3] or perhaps under the low-energy tail of the 2330 Å vibronic transition, as indicated by the profile analysis in Fig. 5. Approximate evaluation of the $G(a_{1g}, a_{2u})$ exchange integral in XeF_2 in a manner similar to that described in the derivation of Eq. (63) indicates that it may be as high as 2 eV. Thus, a fairly large singlet–triplet separation is expected. However, further experimental studies are required to establish this point.

The case of XeF_4 is more complicated. Two weak bands are experimentally observed with intensities of $f=0.009$ and $f=0.003$. The singlet–triplet transition mixes with the corresponding singlet–singlet transition, and its intensity should be enhanced by a heavy atom effect. In the treatment of the spin forbidden transitions in XeF_4, the configuration interaction with higher ^1E_u states was not taken into account. This is not serious as these spin–orbit coupling matrix elements are expected to be mainly determined by the fluorine atom, and will thus be small. A more serious uncer-

TABLE IX. Assignment of the forbidden transitions in XeF_2 and XeF_4.

Molecule	λ(Å)	Assignment	$f_{experimental}$	$f_{estimated}$
XeF_2	2330	$^1A_{1g} \rightarrow {}^1E_{1g}$	0.002	0.001
XeF_4	2280	$^1A_{1g} \rightarrow {}^3E_u$	0.009	0.007–0.013
	2580	$^1A_{1g} \rightarrow {}^1E_g$	0.003	0.001

tainty in the numerical computation is that the estimate of the exchange integral [Eq. (69)] is not reliable. The calculated value of $G=1$ eV leads to a singlet–triplet separation of 2.1 eV as computed from Eq. (51). If we assign the 2280 Å band ($f=0.009$) to the $^1A_{1g} \rightarrow {}^3E_u$ transition, the experimental separation of the ^1E_u and ^3E_u states in XeF_4 is 1.48 eV. It is instructive to consider whether the experimental band separation ($\delta=1.48$ eV) and the oscillator strength ratio ($f_+/f_-=24$) can be accounted for by the intermediate coupling scheme. Using δ (exptl.) and $\xi_{Xe}(5p)=0.75$ eV we get from Eq. (51) $G=0.6$ eV. Hence Eqs. (52) to (55) lead to $f_+/f_-=17$ [i.e., f_- (estimated) $=0.013$] in reasonable agreement with experiment.

The results of these calculations show that the singlet–triplet transition is expected to be about one order of magnitude more intense than the vibronic transition. This would indicate that the stronger band at 2280 Å is the singlet–triplet transition $^1A_{1g} \rightarrow {}^3E_u$ and the weaker band at 2580 Å is the vibronic transition $^1A_{1g} \rightarrow {}^1E_g$. Furthermore, such an assignment is consistent with the fact that the intensities of the vibronic transitions in XeF_2 and XeF_4 are expected to be nearly the same. A summary of the results is shown in Table IX.

The general criteria used in the assignment of forbidden transitions should be briefly considered. The temperature dependence of transition strengths are, in principle, a means for determining the vibronic nature of absorption bands. In this work such evidence was used in the case of XeF_2. But in other cases, experimental difficulties may be considerable. In XeF_4, for instance, the relevant vibrational frequencies are larger than in XeF_2 so that the temperature effect is expected to be smaller. Furthermore, since there are two overlapping weak bands, the error in the profile analysis would be larger than the effect expected. In other cases the relevant band may lie in the experimentally difficult vacuum ultraviolet region. It has been suggested, for instance, that the 1475 Å band in the spectrum of CO_2 is due to the symmetry forbidden transition to a bent $^1B_2$ state.[29] A temperature dependence of the intensity of the vibronically induced $n \rightarrow \pi$ transition in the NO_3^- ion has been reported.[30] However, no theoretical estimate of the expected temperature effect was made.

The temperature dependence of the intensity of the xenon difluoride 2330 Å band was found to be about one-half of that predicted theoretically using the harmonic oscillator approximation. This is not an unprecedented discrepancy. The temperature dependence of the weak $^1A_{1g} \rightarrow {}^1B_{2u}$ band in benzene has very recently been studied by a shock-wave technique.[31] The temperature effect observed in that experiment was also less than that predicted by the harmonic oscillator approximation. Thus, the best fit of the experimental data to the hyperbolic cotangent factor of Eq. (10) is made with the vibrational frequency set equal to 1000 to 1400 cm^{-1}. But it is known that the contribution of the e_{2g}(606 cm^{-1}) vibration is a hundredfold more important than that of the e_{2g}(1595 cm^{-1}) vibration.[32] Similarly, temperature dependence studies of oscillator strengths in transition-metal complexes have shown the same trend.[9–11] The increase in intensity is observed but is less than that described by the hyperbolic cotangent factor.

Singlet–triplet transitions may be identified by the application of the intermolecular heavy atom enhancement effect[15] or by the interaction with a paramagnetic electron acceptor, i.e., oxygen or nitric oxide.[33,34] The intermolecular heavy atom effect is of little use for the present case as the enhancement is quite small.[15] Enhancement of spin-forbidden transitions in XeF_2 and XeF_4 by formation of charge-transfer interactions with O_2 or NO are also not very promising as the ionization potentials of the xenon fluorides are quite high.[3] Besides, chemical decomposition of the xenon fluorides would probably occur.

An independent confirmation of the assignment of the forbidden transitions in the xenon fluorides will be of considerable interest. The most promising technique seems to be that of electron impact spectroscopy as recently applied by Kuppermann and Raff to some simple molecules.[35] This method makes possible an unambiguous discrimination between spin-forbidden and symmetry-forbidden electronic transitions.

ACKNOWLEDGMENTS

We wish to thank Dr. C. Chernick, Dr. J. Malm and Dr. H. Claassen for supplying the samples of XeF_2 and XeF_4. Without their generous help this research could not have been performed. We are grateful to Dr. G. Goodman for several discussions.

This research was supported by the U. S. Air Force Office of Scientific Research. We have also benefited from the use of general facilities provided by the U. S. Atomic Energy Commission and ARPA for materials research at the University of Chicago.

[29] R. S. Mulliken, Can. J. Chem. **36,** 10 (1958).
[30] G. P. Smith and C. R. Boston, J. Chem. Phys. **34,** 1396 (1961).
[31] S. H. Bauer and C. F. Aten, J. Chem. Phys. **39,** 1253 (1963).
[32] F. M. Garforth, C. K. Ingold and H. G. Poole, J. Chem. Soc. **1948,** 505.
[33] D. F. Evans, J. Chem. Soc. **1953,** 345; **1957,** 1351, 3885; **1961,** 1987.
[34] R. Grajower and J. Jortner, J. Am. Chem. Soc. **85,** 512 (1963).
[35] A. Kuppermann and L. M. Raff, J. Chem. Phys. **34,** 2497 (1962).